

EAGL: Enhancement Algorithm based on Gamma Correction for Low Visibility Images

Navleen S Rekhi

Research Scholar¹ & Assistant Professor²
IKG Punjab Technical University, Kapurthala¹
DAV Institute of Engineering & Technology
Jalandhar, Punjab-India²

Jagroop S Sidhu

Associate Professor
Department of ECE
DAV Institute of Engineering & Technology
Jalandhar, Punjab-India

Abstract—Under poor light conditions or improper acquisition settings, the image degrades due to low contrast, poor brightness and suffer poor visual quality of the picture. An enhancement is required to manipulate the scale of pixel intensity for significant improvement in the image. This paper proposed the method of gamma correction with a self-adaptive value in accordance with the intensity scale of the image. After transformation to HSI (hue, saturation and intensity) channel, a multi-scale wavelet transform is implemented on the intensity component of the image. The gamma scale is computed from the combination of reformed scale constant of logarithm function and Minkowski distance measure. Lastly, wavelet based denoising technique is applied to suppress high noise coefficients to improve quality of the image. The proposed method is evaluated in terms of visual appearance, measure of information content, signal to noise ratio, and universal image quality index. It demonstrated that the proposed method showed its efficacy in terms of quality and improved visibility.

Keywords—Low scale intensity images; discrete wavelet decomposition; gamma correction; quality metrics

I. INTRODUCTION

The demand for video surveillance, medical imaging, and extensive photography has tremendously risen the challenges in the enhancement of low intensity images. Low intensity refers to illumination whose physical characteristics don't satisfy the normal image [1]. With improper light conditions and poor acquisition settings of imaging devices, the picture is affected by low contrast [2]. Such images exhibit the narrow distribution of intensity values across the intensity scale and are considered to be under/over-exposure scenes. Explicit exposure consists of a broad range of intensity values grouped narrowly into a narrow intensity range [3]. Fig. 1 displays the image with low luminance where most of its values are at the left portion of the intensity scale. Here, the intensity scale refers to the x-axis of histogram values, and the frequency of occurrence is at the y-axis. So, the intensity values at the darkest region (left portion) reflect the low visibility. Due to poor brightness, the image suffers the loss of texture features that define the content or shape of the image. The texture feature is the spatial variation of brightness across the intensity values of the pixels. With poor texture features, usability in applications like computer vision, medical analysis, and object recognition become difficult to characterize the image. So, the enhancement plays a significant role in adjusting the distribution of intensity values for better visibility in the image.

It involves modifying the intensity value for uniform distribution of pixel values at every pixel position along the intensity scale. Such processing enhances the hidden details and improves the contrast in the image. Also, the transformation to a new scale provides various advantages like suppression of noise, brightness preservation, and sharpening of the edges to make the original image more adaptable to human visual perception. The process of enhancement adjusts the luminance value. Here, the 'luminance' denotes the brightness and intensity in the single-channel obtained from RGB (red, green, and blue) color space. The various modifications had been developed taking both hardware and software methods into account. This paper presented the algorithm based on a software approach to improving picture visibility and overall quality.

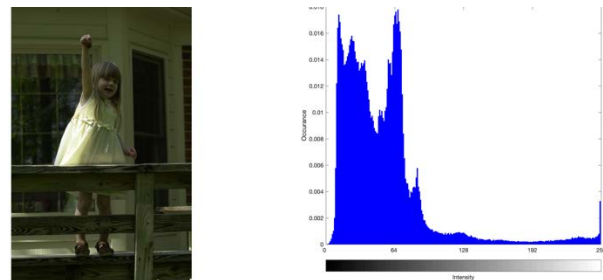


Fig. 1. The Image of Low Intensity Image.

The non-uniformity in an image occurs due to the random distribution of pixel values across the intensity scale. The uniform distribution could be obtained by applying the histogram equalization (HE). It is required to retain the maximal information for improved visibility with optimal quality. But the serious limitation of over-enhancement in HE degrades the quality of an image. Apart from HE, the point processing techniques deliberately balance the non-linear nature of pixel distribution. Most significantly, the gamma correction is the popular approach to produce quality improvement in an image. It is an intensity transformation technique to enhance the image. In simple terms, the input and output are related as: $I_{(u,v)} = I'_{x,y}$, where $I_{u,v}$ and $I_{x,y}$ represent the input and output image. The scale value ' γ ' is the scale factor in gamma correction. It modulates the luminance value to transform the image into better quality. The challenging task in gamma correction is the optimal choice of the scale factor. To overcome limitation of HE, the work is focused to auto-

adjust the scale factor of gamma for the low-intensity image. The scale factor must be automated in such a way to produce better visibility with improved contrast.

The rest of the paper is as follows: Section II discusses the related work on histogram equalization (HE) and other state-of-the-art techniques. Section III presents the key steps to the proposed method, including the conversion to HSI, multi-scale analysis, adaptive gamma correction, and auto-tuning to colour correction. Section IV describes the experimental results evaluated and compared with relevant techniques. Finally, the conclusion is followed by the future scope of the proposed method.

II. RELATED WORK

The piece-wise contrast stretching is the linear approach to scale the brightness. The image with intensity on both sides of the scale (dark and bright) is stretched to obtain the enhanced image. The stretch limit is calculated from the maximum and minimum intensity scale from the reference image. Though the linear stretching method is simple and easy but is entirely suitable for situations in which low and high scales are prominent. So, the non-linear approach of conventional histogram equalization (cHE) is implemented, defined as the frequency distribution technique based on statistical information in the image. The distinct peaks in Fig. 2 displayed the over-enhancement of the low contrast image.

The improved method of cHE based on clipping by mean-median approach on sub-division of HE is commonly used. The approach significantly improved the quality of the over-exposure images. For the image with dark scale values, this method failed to provide scalability in brightness. The MMSICHE[4] sub-divided the image based on median clipped HE. The method claimed to preserve the brightness and information contained in the image. But the method showed its inefficiency in improving the visual appearance of an image. The other method of cHE is the exposure-based sub-regions division of HE, proposed by Tan S and Isa N[2]. The sub-division of cHE in terms of very dark, dark, mid-tone, and lighter regions of a histogram's value were implemented. Most of the pixel values concentrated on the darkest region of the intensity scale. Additionally, Shiguang Liu and Yu Zhang [5] proposed the application of multi-exposure fusion to preserve the detailed information in the image. Other state-of-the-art techniques, such as Brightness Preserving Dynamic-HE (BPDHE) [6], [7] aimed to preserve the mean brightness without severe artifacts. It mapped the sub-histogram into a new dynamic range. The partitions were obtained by calculating the local maximum of the input image. The limitation of this method was that it could not handle the under/overexposed regions in the intensity values. Hence, the modified form of [8] i.e. Fuzzy HE is proposed to overcome the limitation of BPDHE through the implementation of fuzzy crisp values. In the fuzzy-based histogram approach, the partitions were calculated by computing the local maximum. The range of partitions also increased, as the number of pixels count is increased. Since illumination is non-uniform, fuzzy logic lacks a systematic approach to enhance visual appearance. Zuo C. et al [9], [10] proposed a mean-based estimation of object and background from HE. The locally

segmented approach was utilized by Hussain et al. [11] to map the shadow scales over brighter regions. The histogram equalization was implemented by dividing the images into small segments. The process of segmentation was concluded for dark images. If the dark region's scale is variable, over-enhancement could degrade the quality. As a result, the method focused on selecting segments and mapping them to more prominent regions. Recently, dynamic HE [12] was proposed for low illumination MRI images. It followed the same technique of partitions as proposed by previous two methods. Based on a novel multi-scale decomposition, bright regions were separated from dark regions with the domain as non-sub sampled transform. It is a combination of pyramid and directional filter banks. The proposed algorithm had showed the efficacy in handling MRI images. The HE approaches could be effective for natural or for images where pixel distribution is moderate. Most of the HE proposed is focused on preserving the mean brightness and improving the contrast. As shown in Fig. 2, while improving the visual appearance the image is degraded with low contrast. The application of HE and its modified approaches either under-enhanced or degraded the quality of the picture.

The alternate approach of non-linear transformation techniques are gamma correction, logarithmic and exponential function. The sigmoid is an 'S' shaped logistic function that process the image pixel by pixel to enhance the contrast. Srinvas and Bhandari [13] proposed adaptive sigmoid transfer function to achieve enhanced resolution. The sigmoid was utilized as a scale parameter to boost the lower intensity values and adjusted the high intensity values. Similarly, Gupta and Aggarwal [14] proposed a newly developed sigmoid function for contrast improvement in the image. After the transformation to YCbCr model, the normalization parameter was designed using Gaussian based sigmoid function to adjust the illumination. The contrast was enhanced for better colour compensation in the reference image. Other than sigmoid, the transformation of RGB image to extract luminance and chrominance as proposed by Priyanka S et al. [15] used principal component analysis (PCA). Due to direct analysis of raw images, there are colour saturation effects. Hence, the method could not be used for low-intensity images. The improved approach of principal component analysis was suggested by Singh and Bhandari [16]. The authors implemented PCA after the transformation of raw image into HSV channel. This fusion image had a higher quality but with a poor structure similarity index. Also, the global and local contrast adaptive model was proposed by Zhou Z et al. [17] for compensation in brightness. After transformation to HSI, the 'H' component was modified to compensate the low illumination.

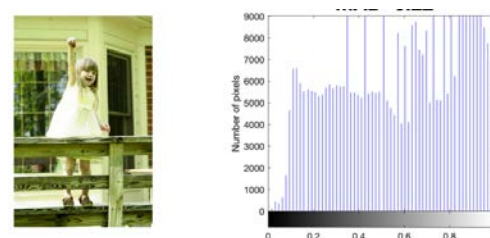


Fig. 2. Histogram Equalization of Low Intensity Image.

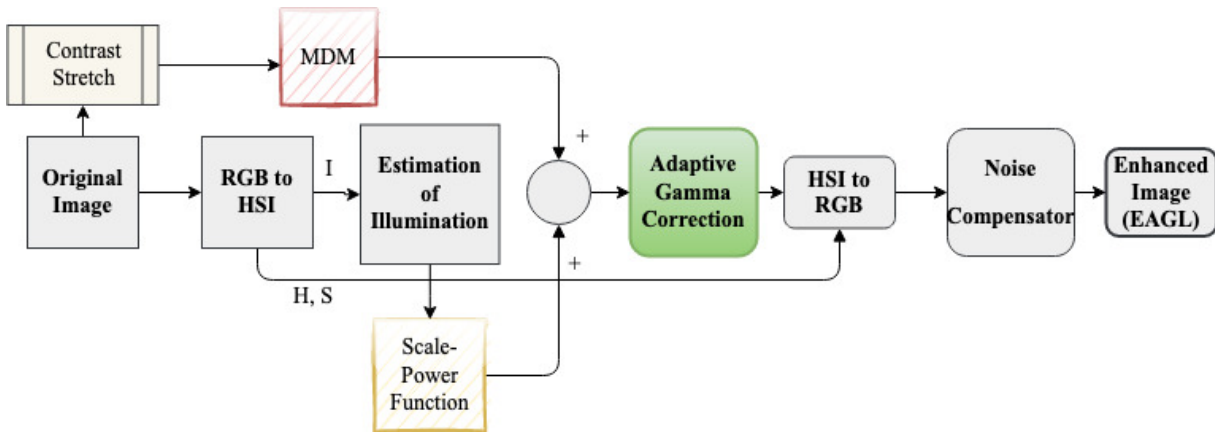


Fig. 3. Flow Diagram of EAGL

Since, the luminance is low, the computed mean could not compensate the poor brightness. Recently, algorithms developed with gamma correction had been the thrust area in image enhancement. The improved gamma correction was developed by Veluchamy and Subramani [16] and computed from cumulative density function. In this method, the detail information was preserved while the contrast was improved. In the previous published work [18], preserving the mean brightness can improve the contrast in the image. Hence, the method was effective for natural and contrast distorted images with moderate intensity values. Rahman S. et al. [19] proposed a mean-based approach to automate the selection of gamma values. The other way was proposed by Parihar [20] and Mahamdioua and Benmohammed [21] to estimate the scale through the computation of entropy and mean of the image. Wang Wencheng [22] proposed an adaptive gamma transform calculated after linear stretching of the corrected brightness in the image. Alternately, the discrete wavelet transform is utilized by Wenyung Yu et al [23] for gamma correction. The illumination was extracted from a low-light image using wavelet decomposition. The contrast value was improved with the computation of global and local spatial illumination. The recent approach for visual correction was proposed with the implementation of principal component analysis (PCA) by Singh and Bhandari [16]. In this approach principal components are adjusted to compute the gamma scale. However, PCA is widely used in image compression. Also, self-adaptive gamma scale was used in the previous work [18]. But the approach was limited to contrast distorted images.

Most of the research is focused on visibility improvement, regardless of simplicity and ease of use. The proposed work is developed to produce simple and effective algorithm for improved visibility. In this paper, multi-scale approach of enhancement is proposed with self-adjustable gamma scale. From the above discussion, the selection of scale parameters plays a significant role in improving the quality of the image. The gamma scale is computed by the combination of the Minkowski distance measure and scale-power (ScP) function. This scale parameter is further used in the gamma correction of the image. To improve the texture features, multi-scale enhancement using 2D discrete wavelet transform is implemented to estimate the intensity component in the image. Finally, the median based noise estimator suppressed high

noise coefficients to minimize the loss of information content in the image.

III. PROPOSED METHOD

A. Flow Diagram (EAGL)

The flow diagram shown in Fig. 3 illustrates the enhancement of low intensity images. It includes two stages: (1) the estimate of illumination and (2) noise correction in the final image. The purpose of the EAGL is to extract detailed information to obtain better visibility of the image. Firstly, the original image is transformed into HSI (hue, saturation and intensity) channel [24]. Mostly, global mean, variance or entropy was used to estimate luminance. Since multi-resolution preserved the maximum amount of detail (energy), a 2D-discrete wavelet transforms at a scale level of '2' [24] is used to obtain luminance value from the intensity component of the input image. The scale value is computed by combining the scale-power function and Minkowski distance measure (MDM) from the contrast stretched and wavelet coefficients of the original image. The combination provided the self-adaptive scale for gamma correction. Finally, threshold-based wavelet shrinking is implemented to suppress any noise artefacts due to transformation in the input image.

B. RGB to HSI Conversion

The image consists of sRGB (standard red, green and blue) combined to form a visual representation. Because of the non-linear nature of true colour, the image is usually transformed into other space channels like HSI [25]. Each of these parameters contains the dominance of wavelength known as hue (H), purity of colour as saturation (S) and the brightness/intensity value (I). The intensity part 'I' in the HSI (shading space) is isolated from and irrelevant to the chrominance part H, i.e., the shading data of a picture. To manipulate a shading picture independently, the 'I' can be improved while keeping the 'S' and 'H' the same. HSI is a 2D representation that approximates the way humans perceive colour. As a result, it retains a higher degree of brightness (for better visual perception). The relation is given as:

$$l_{(x,y)} = \max[R, G, B] \quad (1)$$

Where ' $l_{(x,y)}$ ' is denoted luminance component comprises of maximum intensity of red, green, and blue channel.

As it could be observed from Fig. 4, ‘I’ component is the exact brightness represented in the original image. In our experiments, hue and saturation remained unchanged and intensity value is further processed for image enhancement.

C. 2D-Discrete Wavelet Transform

After transformation to HSI, intensity component is further processed with 2D-discrete wavelet transform (DWT) to down-sample the intensity from the ‘ $l_{(x,y)}$ ’ (refer Eq. 1). The wavelet domain is considered to be high energy compaction tool for image processing. The decomposition in wavelet domain explores the directional variation (horizontal, vertical and diagonal) in image. The image is decomposed at a scale level of two to obtain wavelet coefficients as low-low pass (LL), high-low pass (HL), low-high pass (LH) and high-high (HH). The coefficients of LL are used for computation of scale-power function (as shown in Fig. 5). In our experiments, ‘sym5’ is considered as mother wavelet. The ‘sym5’ is a symmetrical mother wavelet mostly used for the non-linear content in the information.

The Fig. 5 shows the implementation of wavelet transform to separate the luminance from detail coefficients. The 2D-DWT is implemented in row- column form computed from one dimensional DWT. For a given image ‘ $l_{(x,y)}$ ’ is filtered to obtain two ‘ l_a ’ as approximation and ‘ l_d ’ detail (each of size $N \times N/2$ (N is the number of pixels)) coefficients.

The visible region in the Fig. 4 (after 1-level decomposition) is the low-low pass filter coefficients and the other dark portion is the corresponding

$$l_d^i(j',m,n) = \frac{1}{\sqrt{mn}} \sum_{\substack{1 \leq x \leq m \\ 1 < y < n}} L(x,y) d_{j',m,n}^i(x,y) \quad (2)$$

$$l_a(j',m,n) = \frac{1}{\sqrt{mn}} \sum_{\substack{1 \leq x \leq m \\ 1 < y < n}} L(x,y) a_{j',m,n}(x,y) \quad (3)$$

Where ‘ $l_d^i(j',m,n)$ ’ and ‘ $l_a(j',m,n)$ ’ are the detail and approximation coefficients of Eq. 1, j is the scale value. The decomposition is for one scale level and the mother wavelet used is ‘sym5’.

D. Scale-Power Parameter (Sc-P)

From the obtained coefficients at a level of ‘2’, scale value is computed. The value is the modified form of scale constant in logarithmic function. It is well known that logarithmic function is defined by the relation as $s=c \log(1+r)$ [3]. The scaling constant ‘c’ is chosen such that input intensity is mapped to high values and is calculated as: $c = \frac{255}{\log(1+J_m)}$, where ‘255’ is the maximum scale level, ‘ J_m ’ is the maximum intensity in the reference image. The scale constant ‘c’ produces loss of information for higher range of pixel values in the image. So, the proposed method modified the scale constant with the combination scale and power function.

Firstly, the scale is modified into the given relation as:

$$\xi^{ScP} = \frac{[J_m - l_a'(j',m,n)]}{\log(1+l_a'(j',m,n))} \quad (4)$$

ξ^{ScP} is the scale computed from modified scale constant of logarithmic function where in the numerator value is modified

from ‘255’ to $[J_m - l_a(j',m,n)]$ where ‘ J_m ’ is the maximum intensity in the $l_a(j',m,n)$ and $l_a'(j',m,n)$ is the mean computed as: $l_a'(j',m,n) = \sum_{\substack{0 \leq m \leq M-1 \\ 0 < n < N-1}} l_a(j',m,n)$. Similarly, the denominator value is modified to $\log(1+l_a'(j',m,n))$. Next, to avoid the exaggerated intensity variation, ξ^{ScP} is further decimated to the power of 0.005. This value is taken as constant for the images whose intensity scale varies from dark to medium range of pixel distribution.

E. Minkowski Distance Measure (MDM)

For the gamma-based correction, the value of gamma greater than one will increase the intensity of the dark region. Since, the focus of the paper is to scale the intensity in the image, hence ξ^{ScP} is combined with the value of Minkowski distance measure (M^{em}). The M^{em} is a generalized form whose properties are computed from Euclidian and Manhattan distance formula. The final scale value computed for gamma is related as:

$$\gamma = \xi^{ScP} + M^{em} \quad (5)$$

F. Adaptive Gamma Correction

The gamma correction is the non-linear transformation function in which the compression and expansion is attained by changing the value of scale parameter. Finally, the improved gamma correction is implemented with the given relation as below:

$$l_{(x,y)}^{new} = (l_{(x,y)})^{1/\gamma} \quad (6)$$

where $l_{(x,y)}^{new}$ is the newly constructed luminance component of HSI channel.

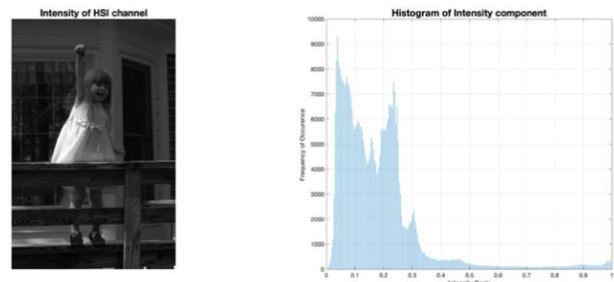


Fig. 4. Representation of ‘I’ Component of the Reference Image.

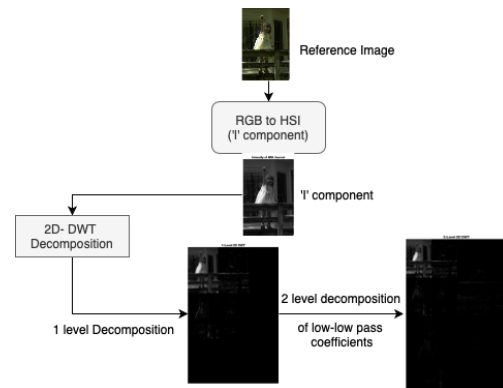


Fig. 5. 2D DWT Decomposition at a Scale Level of ‘2’.

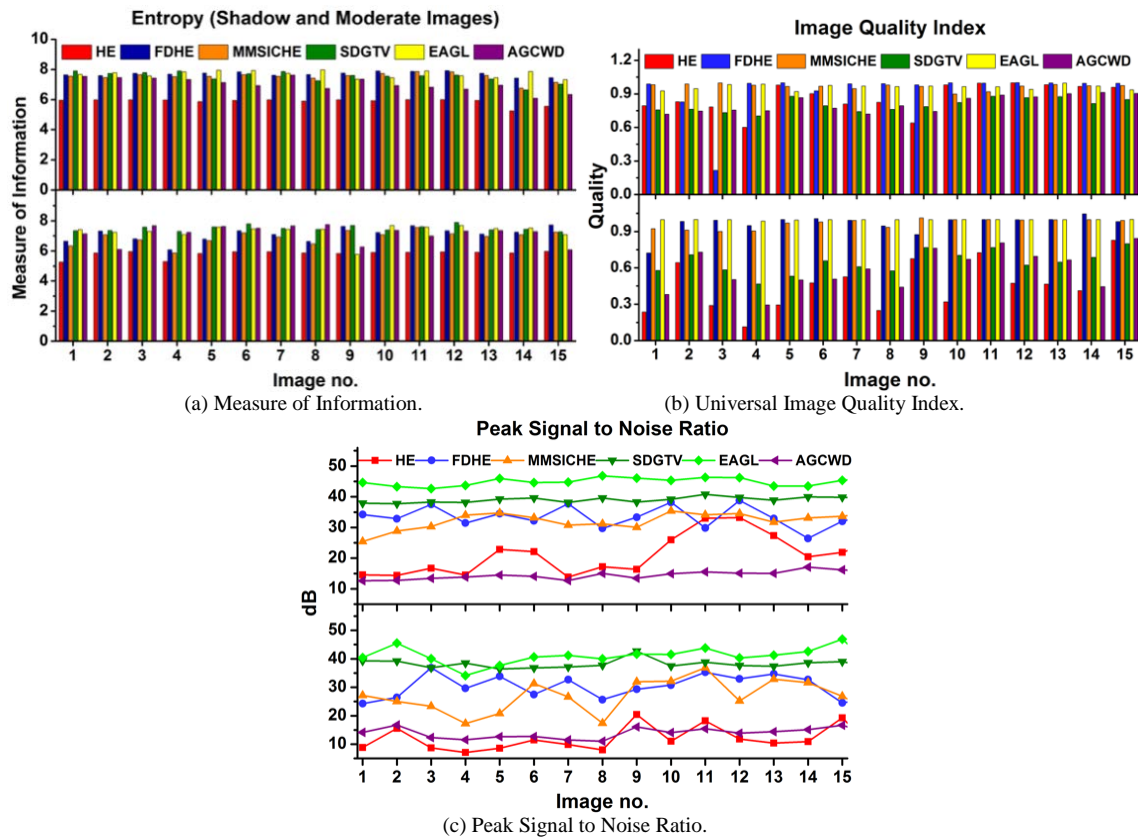


Fig. 6. Comparison of Image Quality Measures (a) Entropy, (b) Universal Image Quality Index and (c) Peak Signal to Noise Ratio for Set of Shadow (Top) and Moderate (Bottom) Images with HE, FDHE, MMSICHE, SDGTV and Proposed Method (EAGL).

G. Noise Compensation

Despite the non-uniform distribution of illumination, the hue contains the dominant wavelength of colours. Before the transformation, the hue component is adjusted from the mean square error. The self-adjusted hue compensation is computed from the mean square error between the reference and contrast stretched image. The new intensity component is transformed back to its original channel space by combining it with other channels. The transformation often degrades the quality of the image. Most of the techniques like median/mean filtering and Gaussian filter often process the noise by individual filtering. Due to high-frequency noise, the final image is blurred near the edges. So, wavelet based de-noising technique is implemented in the proposed method to effectively preserve the quality in the image. With the similar process of multi-scale 2D DWT, the adjusted threshold value is computed (Eq. 7). For any pixel value in the sub-band which is less than the threshold is set to zero and otherwise shift to the other pair of sub-bands. The threshold is calculated by the general equation as:

$$Th = \frac{\sigma^2}{\sigma_{sb}} \quad (7)$$

Where σ^2 is the median estimator computed from the sub-bands and σ_{sb} is the standard deviation of the sub-bands.

The proposed algorithm can be summarized as below:

-
- Input Image:** $l_{(x,y)}$; **Output Image:** $l_{(x,y)}^{new}$
-
- Step I: Transformation of standard (sRGB) image to HSI as given in Eq.1
 - Step II: Decompose the 'I' component using 2D- discrete wavelet transform (keeping saturation unchanged). From Eq. 2 and Eq. 3
 - Step IV: Estimate the scale parameter from image decomposition (Eq. 4) and confidence scale from contrast stretched image (Eq. 5)
 - Step V: Implement gamma correction as stated in Eq. 6 on the luminance component.
 - Step VI: The final enhanced image is obtained after conversion to sRGB channel.
 - Step VII: Perform the noise compensation using Eq. 7 and Eq. 8 to obtain output image as $l_{(x,y)}^{new}$.
-

The value obtained from Eq. 7 is used to suppress the noise coefficients through wavelet based bivariate shrinking [26]. The soft thresholding as stated in Eq. 8 is used to regulate the visibility for better texture features in the image. The Fig. 7 shows the basic illustration of threshold-based noise compensation. Since the noise is at finer level of scales, hence the wavelet coefficients represent the noise at higher scales. So, the soft thresholding scales down the coefficients that are less than the threshold value. After gamma correction, the $l_{(x,y)}^{new}$ is transformed to its original sRGB channel.

$$T^S(w|t) = \begin{cases} 0 & \text{for } |w| \leq t \\ w - t & \text{for } |w| > t \\ w + t & \text{for } |w| < -t \end{cases} \quad (8)$$

$T^S(w|t)$ is the soft-threshold equation. Where 'w' is the wavelet coefficients and 't' is the threshold value.

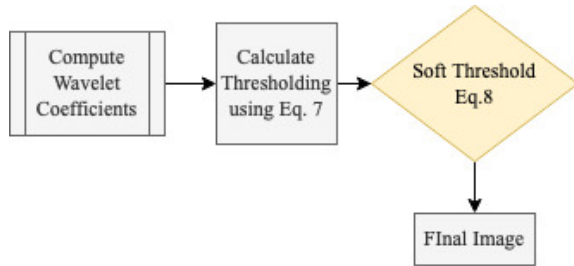


Fig. 7. Process of Wavelet Shrinking.

IV. EXPERIMENTAL RESULTS

In this paper, the experiments were conducted on Intel (R) Core (TM) i5-6th generation with 8 GB of RAM, and the software

A. Image Quality Assessment Measure (IQA)

An objective measure is based on certain criteria to assess the quality of the enhanced image. Although the quantitative metrics are not the perfect way to analyze the quality of enhancement. However, objective evaluation is usually an indicator of image quality. Because with no reference of precise image, the measure of quality is difficult to predict. To the best of our knowledge, there is no IQA method specifically designed to evaluate low-light image enhancement techniques. But, however, such metrics quantify the distortion content in the image. As a result, in various research articles [13], [16], [27], different objective assessment is used to evaluate final image. The quality measure is based on full reference methods and non-referenced methods dependant on reference image. With extensive study of research articles [29], [30], [19], [22] the following metrics were considered for our method. In our metrics, both no-reference and full reference measure had been quantified. The below listed metrics are briefly discussed.

B. Entropy (E)

It is the measure of information content in the resultant image. In cases, like low light images, higher the entropy more will be the information content in the image. With the increase in information, detail of the image too will become finer. The entropy of the image is calculated by the formula:

$$H = - \sum_{i=0}^{L-1} p(i) \log p(i). \quad (9)$$

where H is the entropy, L is the overall gray-scales of image, p(i) is the probability of gray level 'i'.

As per the measure of entropy, the higher the E value, the more information the image contains and the richer would be the image detail.

C. Peak SNR (PSNR)

It quantifies the quality of a reconstructed image with reference to the original image. The final image is compared to input image to estimate the noise content in the information signal. Higher the value of Peak SNR [29], better will be the quality of image. It is calculated from mean square error and is given as:

$$P_{SNR} = 10 \log_{10} \left(\frac{255}{\sqrt{MSE}} \right) \quad (10)$$

where MSE is the mean square error calculated between $l_{(x,y)}$ and $l_{(x,y)}^{new}$

D. Universal Image Quality Index (UIQI)

It is a quality index to measure loss of correlation, luminance and contrast distortion. It is proposed by Wang et al. [31] that quantifies the quality more effectively than mean square error. With the increase in the index value, better will the quality of image.

The visual and histogram representation of some randomly chosen images is shown in Fig. 8. The selected images were divided into three groups, viz. shadow, moderate and low intensity images. For comparison, the random selection of 15 images in each group was chosen. By shadow, it means the images have variational illumination as shown in Fig. 8(b), whereas the moderate images are represented in Fig. 8(c) and Fig. 8(d). And lastly, the low visibility image as illustrated in Fig. 1 and Fig. 8(a). The images shown in Fig. 8 showed the non-uniform distribution of histogram values. Hence, if the intensity scale is widespread, it will degrade the quality of the image. The EAGL enhanced image showed the optimal shifting of scale values to improve the visibility with the desirable amount of contrast. A bell-shaped Gaussian curve could be observed in the 'airport' image. In case of 'shadow' image, the uniform distribution of pixel values is observed. The 'cart' image has dual peaks both at the dark and light scale. The peaks were retained to avoid any loss in detail information and with the shift of intensity scale, visibility is improved. Further, Fig. 6 is the qualitative comparison of shadow and moderate intensity images. In comparison to other well-known algorithms, high PSNR, better quality and preservation of information is found in the proposed method (as summarized in Table I).

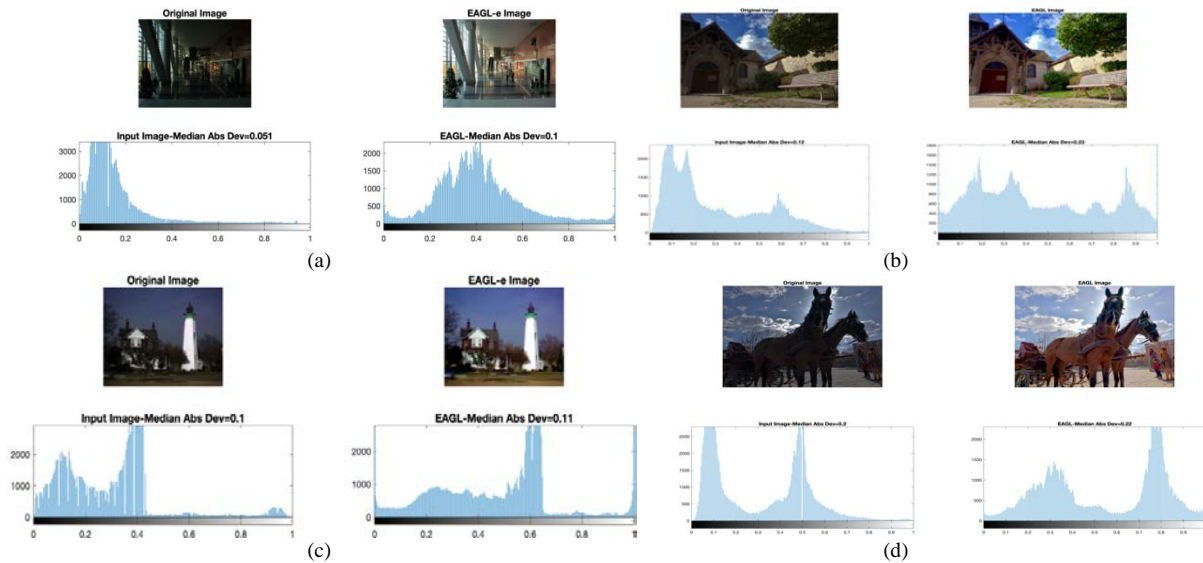


Fig. 8. Results Obtained from Proposed Method (EAGL) for Low Intensity and Low Pixel Counts (a) Airport, (b) Shadow, (c) Farmhouse and (d) Cart.

TABLE I. GROUP COMPARISON OF ALGORITHMS WITH THE PROPOSED METHOD

Group	IQA	HE	FDHE[28]	MMSICHE[4]	SDGTV[32]	AGCWD[33]	EAGL
Shad	E	5.78	7.62	7.42	7.38	6.85	7.64
	PSNR	21.29	33.12	32.40	39.14	14.85	45.18
	UIQI	0.89	0.91	0.96	0.79	0.82	0.96
Mod	E	5.80	7.02	6.82	7.49	7.22	7.36
	PSNR	11.19	29.70	26.41	37.95	13.65	40.69
	UIQI	0.41	0.96	0.96	0.61	0.57	0.99
Low	E	5.14	6.77	6.52	7.36	7.13	7.24
	PSNR	18.27	28.60	23.01	37.94	12.59	40.39
	UIQI	0.78	0.89	0.93	0.56	0.50	0.94

^{Bold indicates better results}

E. Comparison of Enhancement Algorithm with EAGL

The original image (Fig. 1) is a low intensity (mean =46.89) image with the size of 524x800, where the intensity values is concentrated on the left (dark) extrema of the intensity scale. The purpose of enhancement in the image is to scale the hidden details (background and the girl) without introducing any artificial artefacts.

Fig. 10 illustrates the comparison with the classical techniques HE, and the improved HE as developed by [4], [28] and the recent published algorithms by [13], [22], [27]. The fusion-based algorithm developed by Fu et al. [27] had quoted that the ‘girl’ image constituted both bright and dark scale (dress) that had been preserved simultaneously. But with the over enhancement, the image produced is low in sharpness. The HE is the simplest and computationally fast technique to enhance the distorted image. It statistically increases the contrast of the images having detailed intensity values. However, the finished image produced by HE and others related to HE showed poor preservation of details and contrast wrapped in the image. The similar nature of ‘dullness’ and over enhancement could be observed in the recent published

algorithm. Whereas in EAGL, the ‘girl’ in the image and its background had significantly improved the intensity of the low intensity image while preserving the details in the image. Fig. 9 is the histogram representation of enhanced image obtained from EAGL method. The shift in histogram values from dark scale to relatively bright region showed the global improvement in the image. The resultant image of the other HE based approach showed the effects of under and over-exposure of illumination which results in poor contrast. The resultant image of fuzzy-based HE (FDHE) showed under-exposure which results in poor visibility.

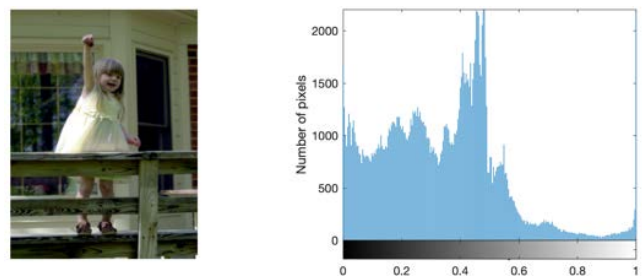


Fig. 9. Enhanced (EAGL) Image.

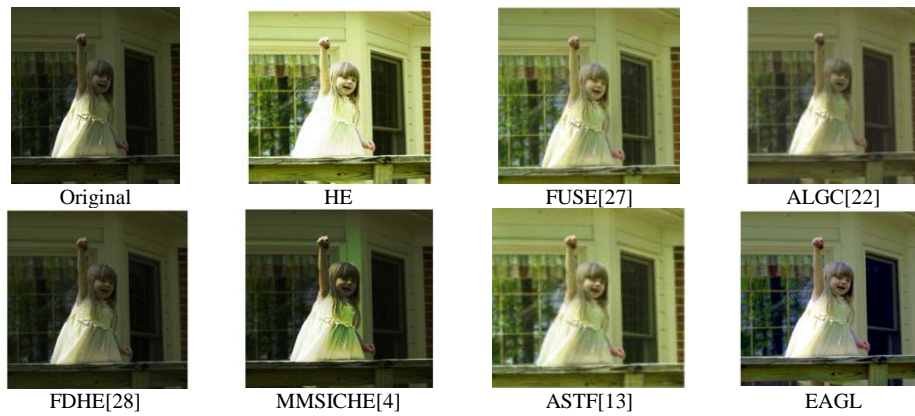


Fig. 10. Comparison of EAGL with the Recent Developed Algorithms based on Low Intensity Images.

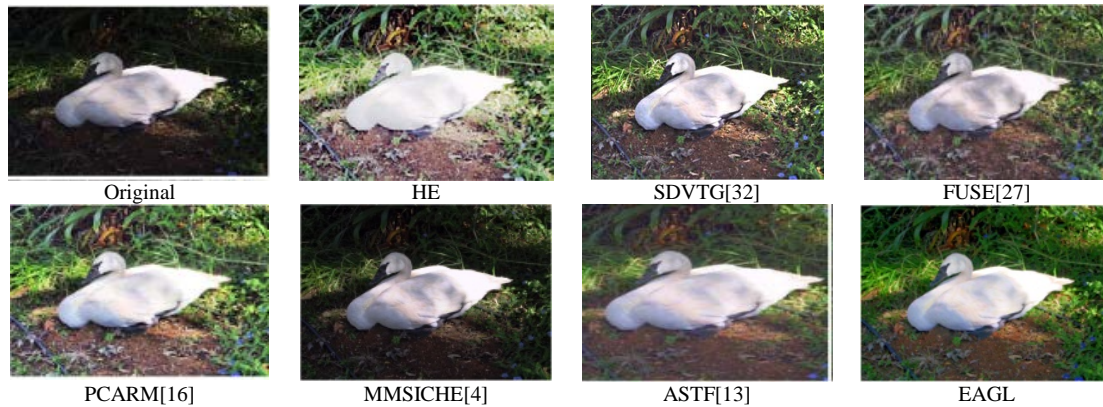


Fig. 11. Comparison of 'Swan' Image with other Relevant Algorithms.



Fig. 12. Comparison of Shadow (House) Intensity Image.

In case of MMSICHE [4], effect of color saturation had degraded the quality of the image. But in case of EAGL, the global brightness is achieved to improve the visual quality and contrast in the image. The steepness in the intensity of the pixels is improved without the loss of information (entropy). With better visibility, the background details in the image (shadow in the glass window) is improved while preserving the contrast color transition from the object with the background, whereas Fig. 12 shows the visual comparison of shadow images. The main criterion of shadow images is to produce a balance between brightness and contrast for a better visual appearance. The compared results were obtained by the default settings of the published algorithms. The method of semi-decoupled decomposition [33] produced over enhancement and degrade the quality of the image. In the case of a fusion-based algorithm [27], the haziness in the image had degraded the

overall appearance in the image. The HE and MMSICHE had not shown any significant improvement in the overall picture. With improved contrast and optimal brightness, high PSNR and quality index proved the efficacy of EAGL.

Table II summarized the comparison of visually compared images shown in Fig. 10, Fig. 11 and Fig. 12. The comparison is made with the standard enhancement technique HE, fusion based and semi-decoupled decomposition method. The proposed method is found to have high PSNR, quality index and better retention of information.

TABLE II. COMPARISON OF IMAGE 'SWAN', 'GIRL' AND 'HOUSE' WITH LOW-LIGHT ALGORITHMS

Image	IQA	SDVTG[32]	FUSE[27]	HE	EAGL
Swan(Figure 11) (513x385)	E	7.27	7.29	5.56	7.32
	UIQI	0.53	0.59	0.39	0.79
	PSNR	37.44	14.94	9.17	41.77
	TIME(sec)	3.20	1.78	0.31	0.40
Girl (Figure 10) (524x800)	E	7.34	7.35	5.95	7.09
	UIQI	0.68	0.47	0.37	0.83
	PSNR	34.01	11.78	8.73	41.09
	TIME(sec)	4.13	2.02	0.43	0.38
House(Figure 12) (1760x1160)	E	7.36	7.43	5.86	7.79
	UIQI	0.86	0.94	0.92	0.95
	PSNR	39.23	17.56	22.84	45.14
	TIME(sec)	21.08	4.02	0.95	0.41

*Bold indicates better results

F. Comparison with Recent Published Methods

Fig. 11 is ‘swan’ image that illustrated the visual comparison of the proposed algorithm with other recent published methods. The different methods were based on multi-fusion, principal component analysis, sigmoid transfer function and other HE based algorithms. The proposed method differs on its effective implementation of gamma and noise compensator. The focus is to devise the method that should be simple and effective to produce better quality in the image. From Fig. 11, the sharpness and the retention of colours produced by the EAGL outperformed the other algorithms. The HE produced over-enhancement and the MMSICHE showed a low luminance image. In case of sigmoid transfer function (ASTF) [13], the image failed to retain the sharpness and thus degraded the quality of the image. The principal component analysis is a dimensionality reduction technique to produce a scaling in brightness. But implementing principal component analysis (PCARM) [16], the loss of details could be visualized near the swan (shadow at the ground) and failed to preserve the variation of shadow to light region. The fusion method [27] lacked sharpness and failed to preserve the detailed information.

Image enhancement is a challenging task in the field of image processing. In continuing efforts of many researchers, the adaptive scale value for gamma correction is proposed. The first abstract the computation of gamma scale using log-power and Minkowski distance measure. The second abstract is the suppression of noise content using a median-based noise estimator and bivariate shrinking. The threshold is computed statistically for the optimal suppression of noise coefficients. Fig. 10, Fig. 11 and Fig. 12 showed the original image and the reconstructed image from the EAGL. The proposed algorithm is designed in a way to effectively enhance the low with a fast response time. The response time and PSNR affects the universal quality of the image.

Table III summarized the result of the proposed method with the algorithms for 100 images in terms of information preservation, quality index, suppression of noise coefficients and the response time.

TABLE III. AVERAGE COMPARISON OF EAGL

Method \ IQA	Entropy	UIQI	PSNR	Response Time (sec)
HE	5.79	0.65	16.24	0.17
SDVTG	6.90	0.67	38.34	0.65
FUSE	7.69	0.92	19.03	2.09
FPDHE	7.13	0.93	30.21	0.43
EAGL	7.36	0.98	46.46	0.29

*Bold indicates better results

V. CONCLUSION

Our experimental results focused on low visibility images due to non-uniform illumination. The prime advantage is (1) improved visibility in texture features, (2) low noise, and (3) improved contrast. In comparison to histogram equalization and other recent algorithms, the self-adaptive gamma scale had shown better improvement in retaining the texture features. The images were chosen in a way that the range of intensity

scale should lie in between extreme low to moderate values. The HE is a simple method but not effective to improve the quality of the image. The other algorithms showed low response time and PSNR which affects the universal quality of the image.

It is concluded that the adaptability to variations in shadow from moderate to low illuminated images is fast in EAGL to produce effective visibility and improved quality.

ACKNOWLEDGMENT

The authors are thankful to IKG Punjab Technical University, Kapurthala and DAV Institute of Engineering & Technology Jalandhar Punjab-India for providing necessary tools and access to peer reviewed journals for successful completion of the work.

REFERENCES

- [1] W. Wang, X. Wu, X. Yuan, and Z. Gao, “An Experiment-Based Review of Low-Light Image Enhancement Methods,” *IEEE Access*, vol. 8, pp. 87884–87917, 2020, doi: 10.1109/ACCESS.2020.2992749.
- [2] S. F. Tan and N. A. M. Isa, “Exposure Based Multi-Histogram Equalization Contrast Enhancement for Non-Uniform Illumination Images,” *IEEE Access*, vol. 7, pp. 70842–70861, 2019, doi: 10.1109/ACCESS.2019.2918557.
- [3] R. C. Gonzalez and R. E. Woods, *Digital Image Processing*. Pearson, 2018. [Online]. Available: <https://www.pearson.com/us/higher-education/program/Gonzalez-Digital-Image-Processing-4th-Edition/PGM241219.html>.
- [4] K. Singh and R. Kapoor, “Image enhancement via Median-Mean Based Sub-Image-Clipped Histogram Equalization,” *Optik (Stuttg)*, vol. 125, no. 17, pp. 4646–4651, 2014, doi: 10.1016/j.ijleo.2014.04.093.
- [5] S. Liu and Y. Zhang, “Detail-preserving underexposed image enhancement via optimal weighted multi-exposure fusion,” *IEEE Transactions on Consumer Electronics*, vol. 65, no. 3, pp. 303–311, 2019, doi: 10.1109/TCE.2019.2893644.
- [6] H. Ibrahim and N. Pik Kong, “Brightness Preserving Dynamic Histogram Equalization for Image Contrast Enhancement,” *IEEE Transactions on Consumer Electronics*, vol. 53, no. 4, pp. 1752–1758, Nov. 2007, doi: 10.1109/TCE.2007.4429280.
- [7] N. S. P. Kong and H. Ibrahim, “Color image enhancement using brightness preserving dynamic histogram equalization,” *IEEE Transactions on Consumer Electronics*, vol. 54, no. 4, pp. 1962–1968, 2008, doi: 10.1109/TCE.2008.4711259.
- [8] V. Magudeeswaran and C. G. Ravichandran, “Fuzzy logic-based histogram equalization for image contrast enhancement,” *Mathematical Problems in Engineering*, vol. 2013, 2013, doi: 10.1155/2013/891864.
- [9] C. Zuo, Q. Chen, and X. Sui, “Range Limited Bi-Histogram Equalization for image contrast enhancement,” *Optik (Stuttg)*, vol. 124, no. 5, pp. 425–431, 2013, doi: 10.1016/j.ijleo.2011.12.057.
- [10] C. Zuo, Q. Chen, X. Sui, and J. Ren, “Brightness Preserving Image Contrast Enhancement using Spatially Weighted Histogram Equalization,” 2014.
- [11] K. Hussain et al., “A histogram specification technique for dark image enhancement using a local transformation method,” *IPSA Transactions on Computer Vision and Applications*, vol. 10, no. 1, 2018, doi: 10.1186/s41074-018-0040-0.
- [12] B. S. Rao, “Dynamic Histogram Equalization for contrast enhancement for digital images,” *Applied Soft Computing Journal*, vol. 89, p. 106114, 2020, doi: 10.1016/j.asoc.2020.106114.
- [13] K. Srinivas and A. K. Bhandari, “Low light image enhancement with adaptive sigmoid transfer function,” *IET Image Processing*, vol. 14, no. 4, pp. 668–678, Mar. 2020, doi: 10.1049/iet-ipr.2019.0781.
- [14] B. Gupta and T. K. Agarwal, “New contrast enhancement approach for dark images with non-uniform illumination,” *Computers and Electrical Engineering*, vol. 70, pp. 616–630, 2018, doi: 10.1016/j.compeleceng.2017.09.007.

- [15] S. A. Priyanka, Y. K. Wang, and S. Y. Huang, "Low-light image enhancement by principal component analysis," *IEEE Access*, vol. 7, pp. 3082–3092, 2019, doi: 10.1109/ACCESS.2018.2887296.
- [16] N. Singh and A. K. Bhandari, "Principal Component Analysis-Based Low-Light Image Enhancement Using Reflection Model," *IEEE Transactions on Instrumentation and Measurement*, vol. 70, 2021, doi: 10.1109/TIM.2021.3096266.
- [17] Z. Zhou, N. Sang, and X. Hu, "Global brightness and local contrast adaptive enhancement for low illumination color image," *Optik (Stuttg)*, vol. 125, no. 6, pp. 1795–1799, 2014, doi: 10.1016/j.ijleo.2013.09.051.
- [18] N. S. Rekhi and J. S. Sidhu, "Adaptive Logarithmic-Power Algorithm for Preserving the Brightness in Contrast Distorted Images," *IJACSA) International Journal of Advanced Computer Science and Applications*, vol. 12, no. 10, pp. 197–205, 2021, [Online]. Available: www.ijacsa.thesai.org.
- [19] S. Rahman, M. M. Rahman, M. Abdullah-Al-Wadud, G. D. Al-Quaderi, and M. Shoyaib, "An adaptive gamma correction for image enhancement," *Eurasip Journal on Image and Video Processing*, vol. 2016, no. 1, pp. 1–13, 2016, doi: 10.1186/s13640-016-0138-1.
- [20] A. S. Parihar, "Entropy-Based Adaptive Gamma Correction for Content Preserving Contrast Enhancement," *International Journal of Pure and Applied Mathematics*, vol. 117, no. 20, pp. 887–893, 2017.
- [21] M. Mahamdioua and M. Benmohammed, "New Mean-Variance Gamma Method for Automatic Gamma Correction," *International Journal of Image, Graphics and Signal Processing*, vol. 9, no. 3, pp. 41–54, Mar. 2017, doi: 10.5815/ijigsp.2017.03.05.
- [22] W. Wang, X. Yuan, Z. Chen, X. Wu, and Z. Gao, "Weak-Light Image Enhancement Method Based on Adaptive Local Gamma Transform and Color Compensation," *Journal of Sensors*, vol. 2021, 2021, doi: 10.1155/2021/5563698.
- [23] W. Yu, H. Yao, D. Li, G. Li, and H. Shi, "Glargc: Adaptive dual-gamma function for image illumination perception and correction in the wavelet domain," *Sensors (Switzerland)*, vol. 21, no. 3, pp. 1–20, 2021, doi: 10.3390/s21030845.
- [24] N. S. Rekhi, J. Singh, J. S. Sidhu, and A. Arora, "Performance Evaluation of Enhancement Algorithm for Contrast Distorted Images," 2022, pp. 29–39. doi: 10.1007/978-981-16-8826-3_4.
- [25] A. Ziemba and E. Fornalik-Wajs, "Time performance of RGB to HSI colour space transformation methods," *Archives of Thermodynamics*, vol. 39, no. 1, pp. 111–128, 2018, doi: 10.1515/aoter-2018-0006.
- [26] A. Dixit and P. Sharma, "A Comparative Study of Wavelet Thresholding for Image Denoising," *International Journal of Image, Graphics and Signal Processing*, vol. 6, no. 12, pp. 39–46, Nov. 2014, doi: 10.5815/ijigsp.2014.12.06.
- [27] X. Fu, D. Zeng, Y. Huang, Y. Liao, X. Ding, and J. Paisley, "A fusion-based enhancing method for weakly illuminated images," *Signal Processing*, vol. 129, pp. 82–96, Dec. 2016, doi: 10.1016/j.sigpro.2016.05.031.
- [28] D. Sheet, H. Garud, A. Suveer, M. Mahadevappa, and J. Chatterjee, "Brightness Preserving Dynamic Fuzzy Histogram Equalization," 2010.
- [29] A. Horé and D. Ziou, "Image quality metrics: PSNR vs. SSIM," *Proceedings - International Conference on Pattern Recognition*, pp. 2366–2369, 2010, doi: 10.1109/ICPR.2010.579.
- [30] Z. Wang, A. C. Bovik, H. R. Sheikh, S. Member, E. P. Simoncelli, and S. Member, "Image Quality Assessment: From Error Visibility to Structural Similarity," vol. 13, no. 4, pp. 1–14, 2004.
- [31] Z. Wang and A. C. Bovik, "A Universal Image Quality Index," 2002. [Online]. Available: <http://anchovy.ece.utexas.edu/~zwang/re>
- [32] S. Hao, X. Han, Y. Guo, X. Xu, and M. Wang, "Low-Light Image Enhancement with Semi-Decoupled Decomposition," *IEEE Transactions on Multimedia*, vol. 22, no. 12, pp. 3025–3038, Dec. 2020, doi: 10.1109/TMM.2020.2969790.
- [33] S. C. Huang, F. C. Cheng, and Y. S. Chiu, "Efficient contrast enhancement using adaptive gamma correction with weighting distribution," *IEEE Transactions on Image Processing*, vol. 22, no. 3, pp. 1032–1041, 2013, doi: 10.1109/TIP.2012.2226047.